

## Crystallographic thermal expansion and elasticity across the superconducting transition in $\text{YBa}_2\text{Cu}_3\text{O}_{7-\delta}$

S. J. Burns, A. Goyal, and P. D. Funkenbusch

*Materials Science Program, Department of Mechanical Engineering, University of Rochester, Rochester, New York 14627*

(Received 17 October 1988)

A thermodynamic treatment for a second-order superconducting phase transformation has been developed which incorporates crystallographic effects. The temperature dependence of x-ray-measured lattice constants in polycrystalline  $\text{YBa}_2\text{Cu}_3\text{O}_{7-\delta}$  has been used to determine the orthorhombic, crystallographic thermal-expansion coefficient matrix. The principal thermal strains were curvefit above and below the superconducting transition temperature to deduce the thermal-expansion jumps at the phase boundary. The thermodynamic arguments show that the three elastic shear stiffness elements do not contribute to the superconducting specific-heat jump. Also, the three independent shear stresses at the superconducting transition point are zero. The specific-heat jump is, however, related to the three normal stresses at the phase boundary. The experimental thermal-expansion data suggest that a compressive stress aligned with the oxygen-deficient crystallographic  $\hat{a}$  axis changes the transition temperature by 0.3 K/kbar; the  $\hat{b}$  axis stress is 0.07 K/kbar, while the  $\hat{c}$  is 0.1 K/kbar, and all stresses are in compression. The isothermal elastic compliance jumps can be predicted by assuming zero jumps in the adiabatic elastic compliances. The specific-heat jump is calculated from this assumption and crystallographic thermodynamics.

### INTRODUCTION

The macroscopic physical properties of the new ceramic superconductors will provide thermodynamic evidence for possible microscopic mechanism(s) of superconductivity (as they did in BCS theory). Further, the pressure dependence of the transition temperature played an important role in finding the  $\text{YBa}_2\text{Cu}_3\text{O}_{7-\delta}$  system from the  $\text{La}_2\text{CuO}_4$ . The new ceramic superconductors have received early attention with respect to the thermodynamics of second-order phase transformations.<sup>1-7</sup> The specific-heat<sup>8-10</sup> and the bulk modulus<sup>11-13</sup> changes were reported across the superconducting transformation temperature. The change in the volume-expansion coefficient across the superconducting transformation temperature has also received preliminary attention.<sup>14-19</sup> The temperature dependence of the lattice spacings, which is the subject of this paper, gives crystallographic information as part of the crystal's thermodynamic response across the normal to superconducting phase transformation boundary.

The relative difficulty of obtaining high-quality, large, single crystals of  $\text{YBa}_2\text{Cu}_3\text{O}_{7-\delta}$  that superconduct, but do not contain twins, has restricted obtaining crystallographic thermodynamic data. The Bi-Sr-Cu-O and the Tl-Ba-Ca-Cu-O systems contain incommensurate lattices (superlattices) and, therefore, give less than ideal crystallographic data. In fact, there are very few reports of crystallographic thermodynamic data even though it is now well accepted that the superconductivity is planar and most properties are strongly anisotropic.

In this paper, the thermodynamic response for a crystal is investigated, in anticipation of the measurements of crystallographic elastic constants. The measurement of the crystallographic thermal-expansion matrix is found.

The crystal's response is found if we assume that the superconducting to normal transformation has no latent heat, i.e., that the crystal's entropy is continuous, and that the crystallographic lattice spacings are continuous. This assumption is identical to considering the transformation to be second order.<sup>3</sup> Using this frame work, the determination of the crystallographic thermal-expansion matrix is then undertaken.

X-ray measurements of the temperature dependence of  $\text{YBa}_2\text{Cu}_3\text{O}_{7-\delta}$  lattice dimensions have previously been reported by Horn *et al.*<sup>14</sup> The values found in this paper are in basic agreement with the neutron-diffraction data of David *et al.*<sup>15</sup> but disagree in detail. It should be noted that the data of Horn *et al.* reduce error bars when compared to the data of David *et al.* Both data sets are, however, at variance with Prokhvatilov *et al.*,<sup>16</sup> who report what appears to be a third-order phase transformation and also at variation with Srinivasan *et al.*,<sup>17</sup> who reported an apparent first-order phase transformation. The superconducting phase change is generally considered as a second-order phase change at the critical point, so only the higher-resolution, second-order data of Horn *et al.* will be considered here.

Ideally, we would like crystallographic data from dilatometer measurements on large, high-quality, superconducting, single crystals. However, the linear thermal-expansion coefficient of polycrystalline  $\text{YBa}_2\text{Cu}_3\text{O}_{7-\delta}$  material has been measured using high-resolution dilatometers<sup>18,19</sup> and these measurements are in basic agreement with the Horn *et al.* thermal-expansion data used in this paper.

Finally, the measured thermal-expansion coefficient matrix jumps will be incorporated into the thermodynamic analysis. This analysis gives the temperature dependence of the stress tensor across the normal to supercon-

ducting phase boundary. Conceptually, the stress tensor describes how the orthorhombic cell of  $\text{YBa}_2\text{Cu}_3\text{O}_{7-\delta}$  must be expanded and contracted to satisfy the second-order, thermodynamic energy balance, across the phase-transformation boundary. An assumption that there are no jumps in the adiabatic elastic compliance matrix is shown to be consistent with some experimental wave propagation data and to *predict* the specific-heat jump.

### CRYSTALLOGRAPHIC THERMODYNAMICS

A second-order, isostructural phase transformation such as the onset of superconductivity, shows continuity of the entropy and each crystallographic cell dimension across the phase boundary. The extensive variables of the crystal are continuous between the normal and superconducting states while the derivatives of these variables have a jump. The incremental internal energy  $dU$  of a crystal per unit mass is changed by the incremental addition of heat and mechanical work:

$$dU = Tds + v\sigma_{ij}d\epsilon_{ij}. \quad (1)$$

$s$  is the entropy per unit mass,  $v$  is the volume per unit mass,  $\sigma_{ij}$  is the applied stress, and  $d\epsilon_{ij}$  is the incremental strain tensor. The incremental strain volume is defined as  $d\Omega_{ij} \equiv vd\epsilon_{ij}$ . The Gibbs free energy of the crystal is

$$G \equiv U - Ts - \Omega_{ij}\sigma_{ij}. \quad (2)$$

From the definition of  $\Omega_{ij}$  and Eqs. (1) and (2), it follows that

$$dG = -sdT - \Omega_{ij}d\sigma_{ij}. \quad (3)$$

$T$  and  $\sigma_{ij}$  are chosen as the independent intensive variables in Eq. (3). The complete crystallographic, thermodynamic description is given below and in the Appendix. This description is based on orthorhombic symmetry operations as described in Ref. 20 while the Voigt notation is used for converting tensor elements to matrix elements. See the Appendix for details.

A first-order phase change has  $G$  continuous across the phase boundary so

$$dG(\text{normal}) - dG(\text{superconducting}) = d(\Delta G) = 0.$$

A second-order phase change has  $d^2(\Delta G) = 0$  across the phase boundary. This condition implies that the second-order components in the  $\Delta G$  expansion have positive and negative terms so that one phase is not always at a lower energy. The second-order components of  $\Delta G$  are formed from the derivatives of  $s$  and the six components of the strain volume. Each of these variables is assumed continuous across the phase boundary implying that no state variable contributes a first-order term. Each component of  $\Delta G$  is zero in this expansion so the sum of the components is also zero. This specifies the phase boundary. The jump conditions on the physical properties are found from this statement of continuity with the aid of the Appendix. First, consider  $s$  to be continuous so

$$s(\text{normal}) - s(\text{superconducting}) = \Delta s = 0.$$

Or

$$d(\Delta s) = \frac{\partial(\Delta s)}{\partial T}dT + \frac{\partial(\Delta s)}{\partial\sigma_1}d\sigma_1 + \frac{\partial(\Delta s)}{\partial\sigma_2}d\sigma_2 + \frac{\partial(\Delta s)}{\partial\sigma_3}d\sigma_3 \\ + \frac{\partial(\Delta s)}{\partial\sigma_4}d\sigma_4 + \frac{\partial(\Delta s)}{\partial\sigma_5}d\sigma_5 + \frac{\partial(\Delta s)}{\partial\sigma_6}d\sigma_6. \quad (4)$$

Reading across the matrix in the Appendix, dividing by  $v$ , letting  $\Delta$  refer to normal less superconducting properties, and noting that  $d(\Delta s) = 0$  gives

$$0 = \frac{\Delta C_\sigma}{T_v}dT + \Delta\alpha_{11}d\sigma_1 + \Delta\alpha_{22}d\sigma_2 + \Delta\alpha_{33}d\sigma_3. \quad (5)$$

Second,  $\Omega_1$  (the tensor element  $\Omega_{11}$ ) is continuous across the boundary so

$$0 = \Delta\alpha_{11}dT + \Delta S_{11}d\sigma_1 + \Delta S_{12}d\sigma_2 + \Delta S_{13}d\sigma_3. \quad (6)$$

Similarly,  $\Omega_2$  and  $\Omega_3$  give

$$0 = \Delta\alpha_{22}dT + \Delta S_{12}d\sigma_1 + \Delta S_{22}d\sigma_2 + \Delta S_{23}d\sigma_3, \quad (7)$$

$$0 = \Delta\alpha_{33}dT + \Delta S_{13}d\sigma_1 + \Delta S_{23}d\sigma_2 + \Delta S_{33}d\sigma_3. \quad (8)$$

Finally, the transformation is isostructural with the shear components of  $\Omega_{ij}$  being zero on both sides of the phase boundary. The changes in  $\Omega_{ij}$  due to shears across the boundary are also zero. The  $\text{YBa}_2\text{Cu}_3\text{O}_{7-\delta}$  crystals in both the normal and superconducting phases are reported as orthorhombic, so these equations will have zeros for the nondiagonal expansion coefficient matrix elements. Thus,  $\Omega_4$ ,  $\Omega_5$ , and  $\Omega_6$  give

$$0 = \Delta S_{44}d\sigma_4, \quad (9)$$

$$0 = \Delta S_{55}d\sigma_5, \quad (10)$$

$$0 = \Delta S_{66}d\sigma_6. \quad (11)$$

These last equations are, to our knowledge, not in the literature and are a direct result of the entropy's stress dependence only appearing in the principal stresses and not on the shear stresses, as seen from the Maxwell relations for shear stress. If a very large residual shear stress were applied to the crystal of  $\text{YBa}_2\text{Cu}_3\text{O}_{7-\delta}$ , there could be a small off-diagonal thermal-expansion coefficient that is nonzero. Such off-diagonal terms might give small  $dT$  contributions in Eqs. (9)–(11). The implication is that the residual shear stress for this case is so large that the orthorhombic crystal cell has become triclinic. In the context of this paper such terms are ignored.

The three independent shear stresses  $\sigma_4$ ,  $\sigma_5$ , and  $\sigma_6$  are eigenvectors for Eqs. (9)–(11). The jumps in the elastic, shear stiffnesses  $\Delta S_{44}$ ,  $\Delta S_{55}$ , and  $\Delta S_{66}$  must be zero across the superconducting to normal phase transformation or else  $d\sigma_4$ ,  $d\sigma_5$ , and  $d\sigma_6$  are zero. If the shear stiffnesses are zero, the result is unexpected since two phonons in three correspond to shear modes and most of the specific heat will be unaffected across the transformation. The interpretation that  $d\sigma$  for shear is zero is reasonable and is as follows: Consider the application of a shear stress,  $\Delta\sigma_6$ , as shown in Fig. 1. Assume, furthermore, that this positive shear stress increases the transition temperature by  $\Delta T_c$ , also a positive value. Now, note that the crystal may be rotated about the  $\hat{b}$  axis by  $180^\circ$ , a twofold rotation. The

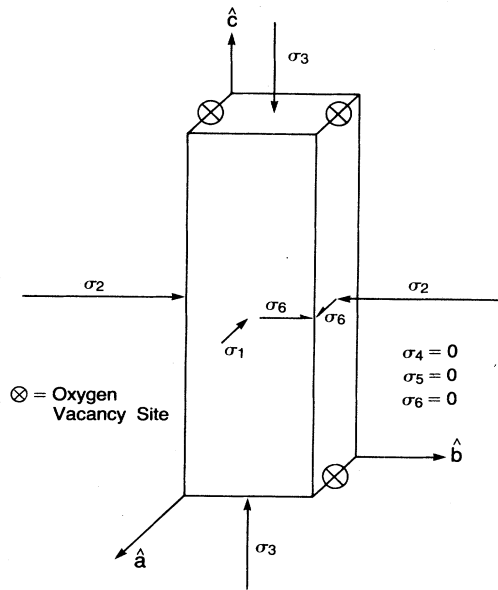


FIG. 1. A crystal of  $\text{YBa}_2\text{Cu}_3\text{O}_{7-\delta}$  with the shear stress  $\sigma_6$  shown. The relative size of the stress components needed for the same change in the transition temperature is from the text for calculating the stress dependence of the phase boundaries.

shear stress in the rotated crystal is now a negative value, but  $\Delta T_c$  is still the same positive value. Thus,  $\Delta T_c$  is increased by both positive and negative shears. It follows that  $dT_c/d\sigma_6 = 0$  when  $\sigma_6 = 0$ . At the critical transition point all the shear stresses are zero and do not couple into the transition temperature. This result is, of course, general and only restricted to being able to change the sign of the shear stress without changing the atomic crystal basis using a twofold rotation axis. The transition temperature is an extremum with all applied shear stresses at zero at the critical point.

Equations (5)–(8) can, at this time, not be solved exactly since the isothermal elastic stiffness jumps for the remaining six elastic stiffnesses have to our knowledge not been measured. However, these equations may be put in matrix form as

$$\tilde{M}d\mathbf{x} = 0, \quad (12)$$

$$\begin{pmatrix} \Delta C_\sigma/vT_c & \Delta\alpha_1 & \Delta\alpha_2 & \Delta\alpha_3 \\ \Delta\alpha_1 & \Delta S_{11} & \Delta S_{12} & \Delta S_{13} \\ \Delta\alpha_2 & \Delta S_{12} & \Delta S_{22} & \Delta S_{23} \\ \Delta\alpha_3 & \Delta S_{13} & \Delta S_{23} & \Delta S_{33} \end{pmatrix} \begin{pmatrix} dT \\ d\sigma_1 \\ d\sigma_2 \\ d\sigma_3 \end{pmatrix} = 0. \quad (13)$$

The phase boundary is the nontrivial solution of (13) that gives an eigenvector for each zero in the determinant of the matrix  $\tilde{M}$ .

### THERMAL STRAINS

Having established a self-consistent crystallographic thermodynamic treatment we will now examine some specific experimental data and its implications. The true

thermal-expansion coefficient, diagonal tensor elements,  $\alpha_{ii}$  for an orthorhombic crystal with  $a$ ,  $b$ , and  $c$  lattice spacings are

$$\frac{1}{a} \frac{\partial a}{\partial T} = \alpha_{11}(T); \quad \frac{1}{b} \frac{\partial b}{\partial T} = \alpha_{22}(T); \quad \frac{1}{c} \frac{\partial c}{\partial T} = \alpha_{33}(T). \quad (14)$$

The crystallographic thermal strains  $\epsilon_{ii}$  are found by integration of Eq. (14) and assigning an arbitrary reference state for zero strain. For example, a reference length  $a^*$  at a temperature  $T^*$  gives

$$\epsilon_{11} = \ln[a(T)/a^*] = \int_{T^*}^T \alpha_{11}(T') dT'. \quad (15)$$

Figure 2 is a plot of the measured  $a(T)$  lattice constant reported as a true thermal strain versus temperature in the superconductor  $\text{YBa}_2\text{Cu}_3\text{O}_{7-\delta}$ . The data were obtained from a powder sample. Pellets of mixtures of  $\text{BaCO}_3$ ,  $\text{CuO}$ , and  $\text{Y}_2\text{O}_3$  were fired at  $950^\circ\text{C}$  for 16 h and slowly cooled to  $400^\circ\text{C}$  in oxygen. The relatively sharp superconducting transition is at 91 K and about 1 K wide. High-resolution x-ray scattering in a Bragg geometry using a rotating anode tube was used to obtain the cell dimensions. The  $\text{CuK } \alpha_1 - \alpha_2$  splitting was fitted by the sum of two Lorentzians. Details are in the original work by Horn *et al.*<sup>14</sup> The data in numerical form were supplied by Held and Keane (see Ref. 14). The reference temperature and lengths have been taken at the lowest temperature for which data were obtained. The slope of each curve in Figs. 2–4 gives  $\alpha_{ii}$ . The orthorhombic crystal has no off-diagonal thermal-expansion terms provided the coordinate system aligns with the crystallographic coordinates.

The thermal strains are relative values and are accurate to about  $\pm 25$  microstrain units. The choice of reference state will change the strain differences between crystal axes but not the thermal-expansion coefficients. The thermal strains on the  $\hat{a}$  axis and  $\hat{c}$  axis show a minimum at low temperatures. This trend is characteristic of type-IV elements and III-V compounds and is seen in other studies of  $\text{YBa}_2\text{Cu}_3\text{O}_{7-\delta}$ .

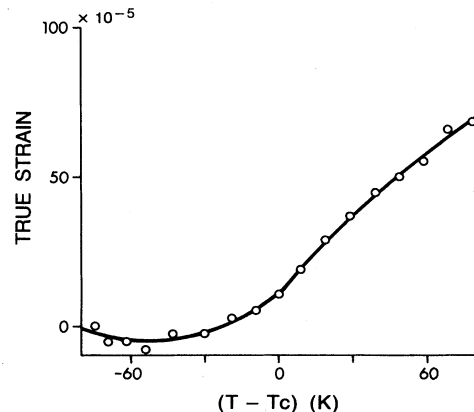


FIG. 2. The thermal strain vs temperature on the  $\hat{a}$  axis. The solid line is a double parabola curve fit. Note the slope difference at the transition.

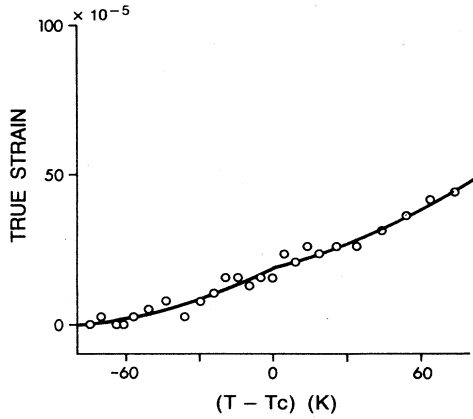


FIG. 3. The thermal strain vs temperature on the  $\hat{b}$  axis. The thermal-expansion coefficient jump is negative.

The thermal strains have been curve fitted to a double parabola that assumes continuity of the thermal strain, i.e., a second-order phase transformation. This piecewise continuous function is used to describe a jump in  $\alpha_{ii}$  should it exist. A first-order transformation would have a jump in the thermal strain values. The form of the thermal strain is found using

$$\epsilon_{ii} = \epsilon_{ii}^0 + C_{ii}^1 \Delta T + C_{ii}^2 (\Delta T)^2. \quad (16)$$

The temperature  $\Delta T$  is measured relative to the superconducting transition temperature at  $T=91$  K. Equation (16) has been used as a piecewise continuous function with  $\epsilon_{ii}^0$ ,  $C_{ii}^1(+)$ ,  $C_{ii}^1(-)$ ,  $C_{ii}^2(+)$ , and  $C_{ii}^2(-)$  chosen so that the difference between the experimental data and the values in Eq. (16) are a minimum. The thermal strain  $\epsilon_{ii}^0$  is from data over the entire temperature range. In the normal state, the data for  $\Delta T > 0$  are fitted and reported as  $C_{ii}^1(+)$ , the superconducting state are reported as  $C_{ii}^1(-)$ . The values of the constants  $C_{ii}^1$  for  $\Delta T > 0$ ,  $\Delta T < 0$ , and  $\epsilon_{ii}^0$  have been optimized from the thermal strain data assuming the statistical noise is in the thermal

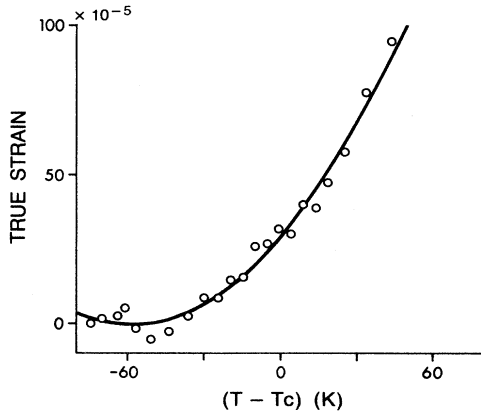


FIG. 4. The thermal strain vs temperature on the  $\hat{c}$  axis. The thermal-expansion coefficient jump is positive but a smaller percentage than either  $\hat{a}$  or  $\hat{b}$ .

TABLE I. Thermal strains  $\epsilon_{ii} = \epsilon_{ii}^0 + C_{ii}^1 \Delta T + C_{ii}^2 (\Delta T)^2$ .

$\Delta T > 0$		$\Delta T < 0$
Normal		Superconducting
$\epsilon_{11}^0$		$10.8 \times 10^{-5}$
$\epsilon_{22}^0$		$18.9 \times 10^{-5}$
$\epsilon_{33}^0$		$28.4 \times 10^{-5}$
$C_{11}^1$	$0.948 \times 10^{-5}/K$	$0.618 \times 10^{-5}/K$
$C_{22}^1$	$0.223 \times 10^{-5}/K$	$0.407 \times 10^{-5}/K$
$C_{33}^1$	$1.113 \times 10^{-5}/K$	$0.989 \times 10^{-5}/K$
$C_{11}^2$	$-2.66 \times 10^{-8}/(K)^2$	$5.93 \times 10^{-8}/(K)^2$
$C_{22}^2$	$1.66 \times 10^{-8}/(K)^2$	$2.09 \times 10^{-8}/(K)^2$
$C_{33}^2$	$6.20 \times 10^{-8}/(K)^2$	$8.51 \times 10^{-8}/(K)^2$

strain, not in the temperature. Finally, the thermal-expansion coefficient jump of normal less superconducting at the transition is just  $\Delta \alpha_{ii} = C_{ii}^1(+)-C_{ii}^1(-)$ . These jumps are found using Eqs. (16), (15), and (14), respectively. The complete set of  $C_{ii}^1$ 's are reported in Table I for each crystal axis.

## RESULTS

The thermal-expansion coefficient matrix  $YBa_2Cu_3O_{7-\delta}$  has been represented by a simple power series near the superconducting transition temperature. The jumps in  $\alpha_{ii}$  at the transition have the  $\hat{a}$  and  $\hat{c}$  axis with positive values while the  $\hat{b}$  axis is negative. The volume thermal-expansion coefficient jump is positive since the sum of  $\alpha$ 's is positive. Recall

$$\frac{1}{v} \frac{\partial v}{\partial T} \Big|_{\sigma_{ij}} = \beta = \frac{\partial}{\partial T} \ln[v(T)/v_0] = \alpha_{11} + \alpha_{22} + \alpha_{33}; \quad (17)$$

$\beta$  is plotted in Fig. 5 by adding the numerical values from Table I. Note in Fig. 5 that there is no attempt to force the thermal expansion coefficients to zero as  $T \rightarrow 0$ . Although, it is realized that this is a requirement of the third

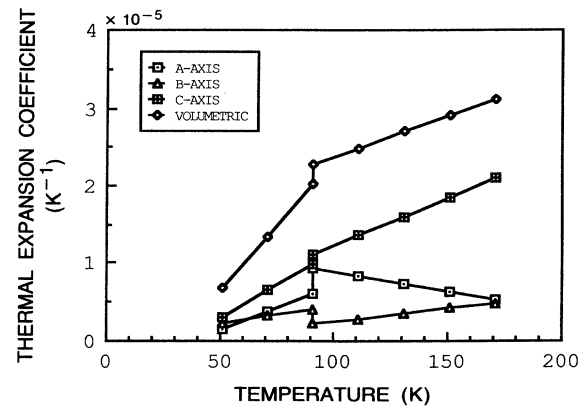


FIG. 5. The curve fit data for showing the contributions to the volumetric thermal-expansion coefficient jump.

law of thermodynamics. The possibility of low-temperature ferroelectric or antiferromagnetic phase changes would make extrapolations to  $T=0$  meaningless. Further, the numerical values for  $\Delta\alpha_{ij}$  are not within the scatter bars for the results of David *et al.* even though their values have very large scatter. In fact, the sign on all the crystal axes is opposite to that obtained here using the data of Horn *et al.* The reasons for this are unclear but may involve differences in sample preparation, chemistry, or microstructure such as twins. (In addition, we are not certain whether the data of David *et al.* was curve fitted to give optimum parabolas as done here.) In this paper we will continue to use the more precise Horn *et al.* data. Assume that  $\Delta S_{11} = \Delta S_{22} = \Delta S_{33}$  and  $\Delta S_{12} = \Delta S_{13} = \Delta S_{23} = -\nu\Delta S_{11}$  with  $\nu=0.3$ . Equation (13) has the following solution using the numerical values:<sup>8-10</sup>  $\Delta C_\sigma/vT_c = -480$  Pa/(K)<sup>2</sup>;  $\Delta\alpha_{11} = 3.3 \times 10^{-6}$ /K;  $\Delta\alpha_{22} = -1.84 \times 10^{-6}$ /K; and  $\Delta\alpha_{33} = 1.24 \times 10^{-6}$ /K. Setting the determinate of  $\tilde{M}$  equal to zero gives  $\Delta S_{11} = -3.4 \times 10^{-14}$ /Pa. Then, Eq. (13) yields the phase boundary as

$$\frac{d\sigma_1}{dT_c} = 120 \text{ MPa/K}, \quad \frac{d\sigma_2}{dT_c} = 4 \text{ MPa/K},$$

and

$$\frac{d\sigma_3}{dT_c} = 74 \text{ MPa/K}.$$

The pressure versus temperature slope is from  $p = -\frac{1}{3} \times (\sigma_1 + \sigma_2 + \sigma_3)$ ,

$$\frac{dp}{dT_c} = -66 \text{ MPa/K}$$

which seems too small<sup>4,5</sup> and of the wrong sign for  $\text{YBa}_2\text{Cu}_3\text{O}_{7-\delta}$ . The strains associated with the stresses

$d\sigma_1$  and  $d\sigma_3$  are expansions of the  $\hat{a}$  and  $\hat{c}$  axis with compressive strains on the  $\hat{b}$  axis due to Poisson's effect.

It should be noted that the jumps are

$$\frac{\Delta S_{11}}{S_{11}} \approx -0.8\%; \quad \frac{\Delta C_\sigma}{C_\sigma} \approx -3\%; \quad \frac{\Delta\alpha_{11}}{\alpha_{11}} \approx 40\%;$$

$$\frac{\Delta\alpha_{22}}{\alpha_{22}} \approx -60\%; \quad \text{and} \quad \frac{\Delta\alpha_{33}}{\alpha_{33}} \approx 10\%.$$

The thermal-expansion jumps are much larger percentages than the predicted elastic stiffness jump and the specific-heat jump. This has implications between isothermal and adiabatic values of the physical, thermodynamic properties as is considered below.

For example, the observation is that the crystallographic wave speeds seem to have no jumps or have jumps that are smaller than can be measured.<sup>21</sup> The jumps in the adiabatic elastic constants, therefore, are also very small. The density is, of course, continuous across the transformation. It will be assumed below that  $\Delta S_{ij}$  adiabatic compliances are zero. The isothermal jumps can now be found from the small difference between isothermal and adiabatic compliances:

$$S_{ij}(T) = S_{ij}(s) + \frac{\alpha_i \alpha_j v T}{C_\sigma}, \quad (18)$$

or

$$\Delta S_{ij}(T) = \Delta S_{ij}(s) + \frac{\alpha_i \alpha_j v T}{C_\sigma} \left[ \frac{\Delta\alpha_i}{\alpha_i} + \frac{\Delta\alpha_j}{\alpha_j} - \frac{\Delta C_\sigma}{C_\sigma} \right]. \quad (19)$$

$\Delta S_{ij}(T)$  in Eq. (19) may be substituted into Eq. (13) and then rearranged to be in a nondimensional form,  $\tilde{M}' d\mathbf{x}'$ . This is done below in anticipation of high precision  $\Delta S_{ij}$  values:

$$\begin{pmatrix} \frac{\Delta C_\sigma}{C_\sigma} & \frac{\Delta\alpha_1}{\alpha_1} & \frac{\Delta\alpha_2}{\alpha_2} & \frac{\Delta\alpha_3}{\alpha_3} \\ \frac{\Delta\alpha_1}{\alpha_1} - \frac{\Delta C_\sigma}{C_\sigma} & \frac{\Delta S_{11}(s)}{\zeta_{11}} + \frac{\Delta\alpha_1}{\alpha_1} - \frac{\Delta C_\sigma}{C_\sigma} & \frac{\Delta S_{12}(s)}{\zeta_{12}} + \frac{\Delta\alpha_1}{\alpha_1} - \frac{\Delta C_\sigma}{C_\sigma} & \frac{\Delta S_{13}(s)}{\zeta_{13}} + \frac{\Delta\alpha_1}{\alpha_1} - \frac{\Delta C_\sigma}{C_\sigma} \\ \frac{\Delta\alpha_2}{\alpha_2} - \frac{\Delta C_\sigma}{C_\sigma} & \frac{\Delta S_{11}(s)}{\zeta_{12}} + \frac{\Delta\alpha_2}{\alpha_2} - \frac{\Delta C_\sigma}{C_\sigma} & \frac{\Delta S_{22}(s)}{\zeta_{22}} + \frac{\Delta\alpha_2}{\alpha_2} - \frac{\Delta C_\sigma}{C_\sigma} & \frac{\Delta S_{23}(s)}{\zeta_{23}} + \frac{\Delta\alpha_2}{\alpha_2} - \frac{\Delta C_\sigma}{C_\sigma} \\ \frac{\Delta\alpha_3}{\alpha_3} - \frac{\Delta C_\sigma}{C_\sigma} & \frac{\Delta S_{13}(s)}{\zeta_{13}} + \frac{\Delta\alpha_3}{\alpha_3} - \frac{\Delta C_\sigma}{C_\sigma} & \frac{\Delta S_{23}(s)}{\zeta_{23}} + \frac{\Delta\alpha_3}{\alpha_3} - \frac{\Delta C_\sigma}{C_\sigma} & \frac{\Delta S_{33}(s)}{\zeta_{33}} + \frac{\Delta\alpha_3}{\alpha_3} - \frac{\Delta C_\sigma}{C_\sigma} \end{pmatrix} \begin{pmatrix} \frac{C_\sigma}{vT} dT \\ a_1 d\sigma_1 \\ a_2 d\sigma_2 \\ a_3 d\sigma_3 \end{pmatrix} = 0 \quad (20)$$

with  $\zeta_{ij} = \alpha_i \alpha_j v T / C_\sigma$  and  $d\mathbf{x}' = C_\sigma / v T dT$ ,  $a_1 d\sigma_1$ ,  $a_2 d\sigma_2$ , and  $a_3 d\sigma_3$ . This nondimensional form shows that the thermal-expansion matrix entries are important for converting measurements of  $\Delta S_{ij}(s)$  into the slopes of  $d\sigma_i/dT_c$  values. Finally, the assumption that  $\Delta S_{ij}(s) = 0$  gives numerical values for  $\Delta S_{ij}(T)$ . The values used in Eq. (19) are<sup>8-10</sup>  $C_\sigma/vT_c = 15.2$  kPa/(K)<sup>2</sup>,  $\Delta C_\sigma/C_\sigma = -0.0315$ ; the thermal-expansion data already found in this paper are  $\alpha_1 = 7.83 \times 10^{-6}$ /K,  $\Delta\alpha_1/\alpha_1 = 0.421$ ;  $\alpha_2 = 3.15 \times 10^{-6}$ /K;  $\Delta\alpha_2/\alpha_2 = -0.584$ ;  $\alpha_3 = 10.51 \times 10^{-6}$ /K,  $\Delta\alpha_3/\alpha_3 = 0.118$ ; so  $\Delta S_{11} = 35.2$ ;  $\Delta S_{22} = -7.42$ ;  $\Delta S_{33} = 19.4$ ;  $\Delta S_{12} = -2.1$ ;  $\Delta S_{13} = 30.9$ ;  $\Delta S_{23} = -9.5$  all in

units of  $10^{-16}$ /Pa. Substituting  $\Delta S_{ij}$  and  $\Delta\alpha_i$  values into the determinate of  $\tilde{M} = 0$  gives  $\Delta C_\sigma/vT_c = -477$  Pa/(K)<sup>2</sup> (see measured value above) with  $d\sigma_1/dT_c = -310$  MPa/K;  $d\sigma_2/dT_c = -1360$  MPa/K; and  $d\sigma_3/dT_c = -810$  MPa/K; so  $dp/dT_c = 826$  MPa/K or the inverse is 0.12 K/kbar. These stresses are shown in Fig. 1. This last value is in reasonable agreement with the measured pressure dependence of the transition temperature.<sup>4,5</sup>

The assumption that the adiabatic elastic compliances do not contribute to the isothermal elastic compliance jumps predicts the jump in the specific heat, the pressure dependence of the transformation, and preliminary data

on the absence of wave-speed jumps in these crystals.<sup>21</sup> Finally, it should be noted that the "correction" from isothermal to adiabatic elastic compliances is typically several percent. The jumps in the isothermal compliances are less than 1% while the thermal-expansion jumps are a much larger percentage. Thus, it seems that the large percentage of the small number is the major contributor to the thermodynamic jumps.

The conclusion to be drawn if  $\Delta S_{ij}(s)$  does, indeed, not directly contribute to the transition is simple: The mechanical part of the lattice represented by  $S_{ij}$  is not

directly participating in the superconductivity.

#### ACKNOWLEDGMENTS

The cooperation of G. Held and D. Keane at IBM Yorktown is appreciated. This work is supported by the National Science Foundation Grant No. MSM-8718693.

#### APPENDIX

The following are definitions using the Gibbs function in Eq. (2):

$$T \frac{\partial s}{\partial T} \Big|_{\sigma_{ij}} \equiv C_{\sigma} = \text{specific heat at constant stress.}$$

$$\frac{1}{v} \frac{\partial \Omega_{ij}}{\partial T} \Big|_{\sigma_{ij}} = \frac{\partial \epsilon_{ij}}{\partial T} \Big|_{\sigma_{ij}} = \alpha_{ij} = \text{thermal expansion coefficient.}$$

$$\frac{1}{v} \frac{\partial \Omega_{ij}}{\partial \sigma_{kl}} \Big|_{T, \sigma'_{kl}} = \frac{\partial \epsilon_{ij}}{\partial \sigma_{kl}} \Big|_{T, \sigma'_{kl}} = S_{ijkl} = \text{isothermal elastic compliance (tensor element).}$$

All tensor elements are reduced to matrix elements using  $11 \rightarrow 1$ ;  $22 \rightarrow 2$ ;  $33 \rightarrow 3$ ;  $23, 32 \rightarrow 4$ ;  $13, 31 \rightarrow 5$ ; and  $12, 21 \rightarrow 6$ . The matrix  $S_{mn}$  is assumed to show orthorhombic symmetry.

	$\frac{\partial}{\partial T} \Big _{\sigma}$	$\frac{\partial}{\partial \sigma_1} \Big _{T, \sigma'_1}$	$\frac{\partial}{\partial \sigma_2} \Big _{T, \sigma'_2}$	$\frac{\partial}{\partial \sigma_3} \Big _{T, \sigma'_3}$	$\frac{\partial}{\partial \sigma_4} \Big _{T, \sigma'_4}$	$\frac{\partial}{\partial \sigma_5} \Big _{T, \sigma'_5}$	$\frac{\partial}{\partial \sigma_6} \Big _{T, \sigma'_6}$
G	$-s$	$-\Omega_1$	$-\Omega_2$	$-\Omega_3$	$-\Omega_4$	$-\Omega_5$	$-\Omega_6$
$s$	$c_{\sigma}/T$	$v\alpha_{11}$	$v\alpha_{22}$	$v\alpha_{33}$	0	0	0
$\Omega_1$	$v\alpha_{11}$	$vS_{11}$	$vS_{12}$	$vS_{13}$	0	0	0
$\Omega_2$	$v\alpha_{22}$	$vS_{12}$	$vS_{22}$	$vS_{23}$	0	0	0
$\Omega_3$	$v\alpha_{33}$	$vS_{13}$	$vS_{23}$	$vS_{33}$	0	0	0
$\Omega_4$	0	0	0	0	$vS_{44}$	0	0
$\Omega_5$	0	0	0	0	0	$vS_{55}$	0
$\Omega_6$	0	0	0	0	0	0	$vS_{66}$

This matrix is symmetric because the second derivatives of the Gibbs free energy are independent of the order in which the derivatives are taken, Maxwell's relations.

<sup>1</sup>C. W. Chu, P. H. Hor, R. L. Meng, L. Gao, Z. H. Huang, and Y. Q. Wang, Phys. Rev. Lett. **58**, 405 (1987).

<sup>2</sup>P. H. Hor, L. Gao, R. L. Meng, Z. J. Huang, Y. Q. Wang, K. Forster, J. Vassiliou, C. W. Chu, M. K. Wu, J. R. Ashburn, and C. J. Torng, Phys. Rev. Lett. **58**, 911 (1987).

<sup>3</sup>S. J. Burns, J. Mater. Res. **4**, 33 (1989); **4**, 458 (1989).

<sup>4</sup>H. Yoshida, H. Morita, K. Noto, T. Kaneko, and H. Fujimori, Jpn. J. Appl. Phys. **26**, L867 (1987).

<sup>5</sup>R. Griessen, Phys. Rev. B **36**, 5284 (1987).

<sup>6</sup>Y. Akahama, S. Endo, S. Noguchi, and K. Okuda, Jpn. J. Appl. Phys. **26**, L871 (1987).

<sup>7</sup>H. A. Borges, R. Kwok, J. D. Thompson, G. L. Wells, J. L. Smith, Z. Fisk, and D. E. Peterson, Phys. Rev. B **36**, 2402 (1987).

<sup>8</sup>M. V. Nevitt, G. W. Crabtree, and T. E. Klippert, Phys. Rev. B **36**, 2398 (1987).

<sup>9</sup>S. E. Inderhees, M. B. Salomon, T. A. Friedmann, and D. M. Ginsberg, Phys. Rev. B **36**, 2401 (1987).

<sup>10</sup>R. A. Fisher, I. E. Gordon, and N. E. Phillips, J. Supercond. (to be published).

<sup>11</sup>D. J. Bishop, A. P. Ramirez, P. H. Gammel, B. Battlog, E. A. Rietman, R. J. Cava, and A. J. Mills, Phys. Rev. B **36**, 2408 (1987).

<sup>12</sup>A. Miglari, Ting Chen, B. Alove, and G. Grüner, Solid State Commun. **63**, 827 (1987).

<sup>13</sup>H. Ledbetter, J. Metals **40**, 24 (1988).

<sup>14</sup>P. M. Horn, D. T. Keane, G. A. Held, J. L. Jordan-Sweet, D. L. Kaiser, F. Holtzberg, and T. M. Rice, Phys. Rev. Lett. **59**, 2772 (1987).

<sup>15</sup>W. I. F. David, P. P. Edwards, M. R. Harrison, R. Jones, and C. C. Wilson, Nature (London) **331**, 245 (1988).

<sup>16</sup>A. I. Prokhvatilov, M. A. Strzhemechnyi, A. P. Isakina, A. S.

- Baryl'nite, and V. V. Demirskii, *Fiz. Nizk. Temp.* **13**, 1098 (1987) [*Sov. J. Low Temp. Phys.* **13**, 625 (1987)].
- <sup>17</sup>R. Srinivasan, K. S. Girirajan, V. Ganesan, V. Radhakrishnan, and G. V. SubbaRao, *Phys. Rev. B* **38**, 889 (1988).
- <sup>18</sup>G. Sparn, W. Schielbeling, M. Lang, R. Held, U. Gottwick, F. Steglich, and H. Rietschel, *Physica C* **153-155**, 1010 (1988).
- <sup>19</sup>E. du Tremolet de Lacheisserie, B. Baraba, and J. H. Henry, *J. Magn. Magn.* **71**, L125 (1988).
- <sup>20</sup>J. F. Nye, *Physical Properties of Crystals* (Oxford Univ. Press, London, 1964), p. 178.
- <sup>21</sup>M. Saint-Paul, J. L. Tholence, P. Monceau, H. Noel, J. C. Levet, M. Potel, P. Gougeon, and J. J. Capponi, *Solid State Commun.* **66**, 641 (1988).